7-2020

A Novel Tri-Band Reconfigurable Microstrip Patch Antenna

Wen Tao Li
Xidian University

Meng Wei
Xidian University

Bahareh Badamchi
Boise State University

Harish Subbaraman
Boise State University

Xiaowei Shi
Xidian University

Wen Tao Li*, Meng Wei, Bahareh Badamchi, Harish Subbaraman and Xiaowei Shi

A novel tri-band reconfigurable microstrip patch antenna

https://doi.org/10.1515/freq-2019-0130
Received August 12, 2019; accepted March 10, 2020; published online April 8, 2020

Abstract: In this paper, a novel tri-band reconfigurable patch antenna with simple structure is presented. By changing the on-off state of only two PIN diodes, the antenna can operate in three bands, namely X-band, Ku-band, and Ka-band. The overall size of the antenna is $0.24\lambda_L \times 0.5\lambda_L \times 0.019\lambda_L$, where λ_L is the free-space wavelength of the lowest operating frequency. A prototype is fabricated and measured to verify the design. The measurement results are in good agreement with the simulation results, which indicate that the proposed antenna can be flexibly switched between three bands of 10.9–11.18 GHz, 15.65–15.9 GHz, and 32.3–33.6 GHz with stable radiation patterns.

Keywords: frequency reconfigurable antenna (FRA); Ka-band; Ku-band; PIN diodes; X-band.

1 Introduction

As a device for transmitting and receiving electromagnetic waves, antenna is an indispensable part of modern wireless communication systems. In recent years, in order to adapt to the rapid development of communication systems, radar, and wireless communication technologies, reconfigurable antennas have emerged as promising candidates [1–3]. Reconfigurable antennas have attracted a great deal of attentions by researchers, due to their advantages, such as small size, multiple functions, and easy to implement diversity applications [4–6]. Antenna frequency, pattern, and polarization reconfiguration have been attempted by utilizing PIN diodes [7, 8], RF MEMS [9, 10], or GaAs switches [11, 12] to change the physical structure of the antenna.

Frequency reconfigurable antennas capable of switching over multiple frequencies or frequency bands have been reported in literatures [13–16]. In [13], a frequency reconfigurable square ring slot antenna is proposed. Due to the small gap between the configured slots, the span of the three bands is small. In [14], a new frequency-reconfigurable bow-tie antenna is proposed. It only achieves frequency reconfigurability in the low frequency band, and also owns a narrow frequency span. In [15], a frequency reconfigurable microstrip antenna using PIN diodes as switches is proposed. By arranging the diode switches on the floor groove, reconfigurability over eight different frequencies is achieved by controlling the on-off states of four switches. However, the size of the antenna connected to the switch is small and can only be reconfigurable within a narrow frequency range. In [16], a frequency reconfigurable quasi-Sierpinski dipole antenna is proposed. By controlling the on and off states of the two pairs of switches loaded on the dipole arms, the antenna can switch between X-band, Ku-band, and Ka-band. A dual-band high impedance surface (HIS) is proposed as an artificial magnetic conductor (AMC) reflector for the antenna. This method reduces the profile height to a certain extent, but lengthens the transverse dimension and complicates the antenna design. In particular, for the Ka-band state, the overall profile is still relatively high and the size is large.

Microstrip patch antennas are prevalent in literatures as a popular candidate for antenna designers for high frequency operation. They are characterized by low profile, light weight, low cost, and easy compatibility with printed circuits, making them attractive for designing high frequency antennas.

In this paper, a simple and novel tri-band reconfigurable microstrip patch antenna based on the PIN diodes is presented. The antenna is printed on one side of the substrate and fed through a conventional SMA connector. By controlling the states of two switches, the antenna can operate in three frequency bands, namely X-band, Ku-band, and Ka-band. A frequency reconfigurable antenna prototype with bias lines is fabricated and tested. Simulated and measured results are provided to verify the

***Corresponding author: Wen Tao Li**, Science and Technology on Antenna and Microwave Laboratory, Xidian University, Xi'an, PR China; and Science and Technology on Electromechanical Dynamic Control Laboratory, Xi'an, PR China, E-mail: wtli@mail.xidian.edu.cn
Meng Wei and Xiaowei Shi: Science and Technology on Antenna and Microwave Laboratory, Xidian University, Xi'an, PR China
Bahareh Badamchi and Harish Subbaraman: Department of Electrical and Computer Engineering, Boise State University, Boise, USA

efficiency of the proposed design. The experimental results show that the proposed design has good reconfigurability.

2 Antenna design and analysis

The proposed frequency reconfigurable patch antenna geometry is illustrated in Figure 1. The antenna is designed on Rogers RO4350 substrate (εr = 3.66 and tanδ = 0.004) with a thickness of 0.508 mm. The overall size of the antenna is 20 mm × 24 mm × 0.508 mm. It consists primarily of a radiating patch, two PIN diodes, a conventional SMA connector and a short-circuited wall, wherein the radiating patch includes a center patch and two parasitic patches (P1 and P2) on both sides. The center patch consists of a circular patch and two concave patches on both sides, which are connected by a rectangular strip and a capacitor. Two PIN diodes are placed between the center patch and the two parasitic patches (P1 and P2). By controlling the on-off state of two PIN diodes, three different operating states can be formed. Generally, the length of the antenna radiating patch is about 0.5λ, λ is the wavelength corresponding to the center frequency. The geometric parameters of the proposed antenna are listed in Table 1. Among them, the center point of the center patch is point O, and the exact location of feed point (probe) is point A. Thus, the vector $\vec{OA}$ is (0.9, −0.8), whose unit is mm.

A short-circuited wall is introduced at the short-side edge of the parasitic patch P2, and the parasitic patch P2 is connected to the grounding plate through the short-circuited wall, which may lead to a larger structural difference in comparison with the conventional microstrip antenna. Hence miniaturization can be achieved on the one hand; On the other hand, the effective inductance of the whole antenna can be increased. The X-band reconfigurability can be achieved by loading a short-circuited wall. Simulated S11 results of the antenna with and without short-circuited wall loading are shown for comparison in Figure 2. It can be seen from the results that the resonant frequency moves from 14.6 to 11.3 GHz and the S11 minima decreases from −13 dB to −24 dB after loading the short-circuited wall, demonstrating considerable improvement in impedance matching.

To achieve reconfigurability of the frequency, we need to change the effective electrical length of the proposed antenna. Therefore, two PIN diodes (MA4AGFCP910 switch from M/A-COM Inc) with a forward bias voltage of 1.33V are employed. The on-off equivalent circuit of PIN diode is shown in Figure 1 (c). When the diode is turned on, it is equivalent to a small resistance. When the diode is turned off, it is

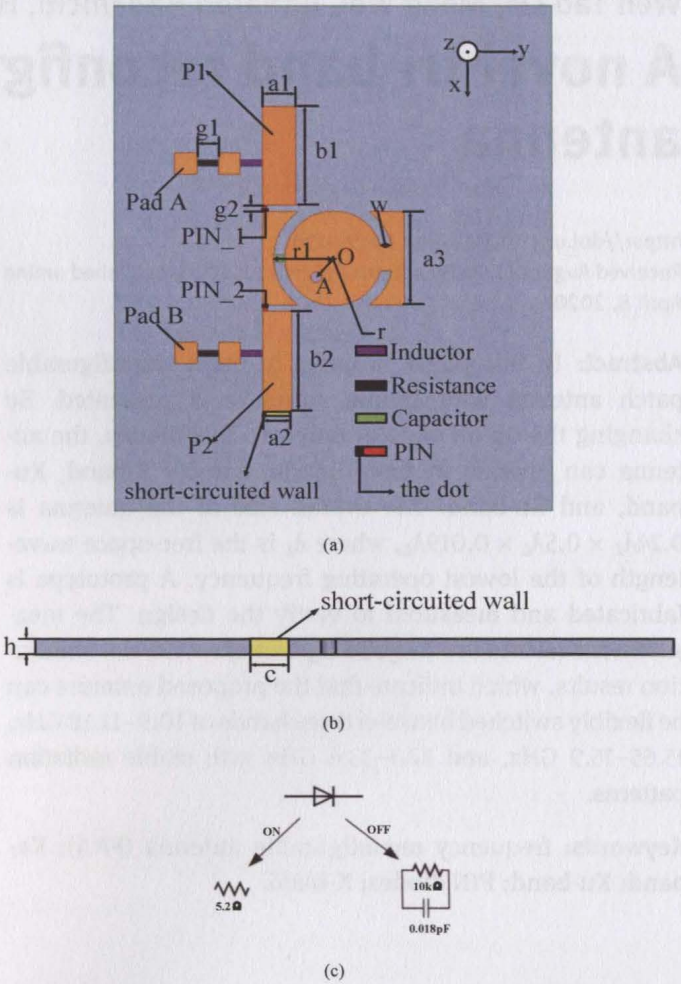

Figure 1: Geometry of the proposed antenna. The dot represents the negative pole of the diode. (a) Top view, (b) Side view, and (c) Equivalent circuit model of diode.

equivalent to the parallel connection of the resistance and the capacitance. When the diode PIN_1 is OFF and PIN_2 is ON, the center patch is connected to the parasitic patch P2 and has a certain coupling effect with P1, which is called State 1. In this state, the antenna works in the X-band. This coupling is mainly due to the small size of the PIN diode and a small distance between the center patch and the parasitic patch. When the diode PIN_1 is ON and PIN_2 is OFF, the center patch is connected to the parasitic patch P1 and coupled with P2, which is called State 2. In this state, the antenna operates in the Ku-band. When the diode PIN_1 is OFF and PIN_2 is

Table 1: Dimensions of the antenna (unit: mm).

a1	*b1*	*a2*	*b2*	*a3*	*g1*
1.5	4.7	1.3	4.8	4.4	1
g2	*w*	*r*	*h*	*c*	*r1*
0.3	0.5	2.25	0.508	1.2	5.5

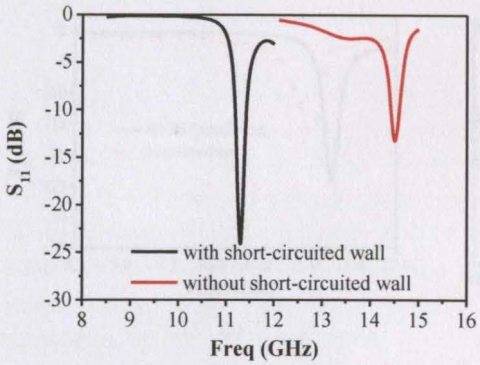

Figure 2: Simulated reflection coefficients (S_{11}) of the proposed antennas with and without the short-circuited wall.

Table 2: Pin diode states and operating band for the three pattern states.

State	Pin_1	Pin_2	Frequency
1	OFF	ON	X-band
2	ON	OFF	Ku-band
3	OFF	OFF	Ka-band

OFF, the center patch is not connected to the two parasitic patches, which is called State 3. In this state, the antenna operates in the Ka-band. These three states, together with their PIN diode states, are summarized in Table 2.

To further illustrate the reconfigurability, the surface current distribution in three states of the antenna operation is shown in Figure 3. As can be observed from Figure 3 (a), at state 1, the current is mainly distributed on the center patch and parasitic patch P2, and there is almost no current on the parasitic patch P1. As shown in Figure 3 (b), at state 2, the current is concentrated on the center patch and the parasitic patch P1, and almost no current flows through the parasitic patch P2. With reference to Figure 3 (c), at state 3, most of the current is in the central patch. Due to the coupling effect with the parasitic patches P1 and P2, there is also a small amount of current distribution on P1 and P2. In summary, the current distribution in Figure 3 illustrates the reconfigurability of the antenna very well.

In addition, in order to provide DC bias to the diode and reduce the influence of DC current and lumped parameter components on the radiation characteristics of the antenna, a simple feed network is also integrated on the dielectric plate. The capacitors and inductors are loaded to avoid interference between the DC source and the RF AC source. The resistor is loaded to prevent the PIN diode from being burnt out due to excessive DC voltage. The actual feed system is substituted into the entire antenna. The design process optimizes the impedance matching of the antenna, making the simulation results of the antenna closer to the measured results. The proposed frequency reconfigurable patch antenna with a simple feed network geometry is illustrated in Figure 1. Pads A and B are connected to the positive bias voltages (V1 and V2).

To get a deep insight into the proposed antenna, we have carried out an investigation on its related parameter. Here, the width of the center patch, the length of two parasitic patches and the radii of sector parts of the center patch are examined by Ansys HFSS. Figure 4 (a) illustrates the effect of the width of the center patch (a3) on the reflection coefficient (S11). With an increase in a3, the current path on the center patch also increases. Hence, the resonant point shifts to the lower frequency band. Similarly, from Figure 4 (b), we can see that when the length of parasitic patch P1 (b1) increases, the resonant frequency also shifts to the lower frequency band. Figure 4 (c) shows the effect of the length of parasitic patch P2 (b2) on the reflection coefficient (S11). As the value of b2 is tuned slightly, a noticeable change on the impedance matching and the resonant frequencies can be observed. In particular, we can see that impedance characteristics become better with increasing values of b2. Through scanning these parameters, we arrived at optimized values for a3, b1, and b2 as 4.4, 4.7, and 4.8 mm, respectively. Finally, it can be seen from Figure 4 (d) that, as the radii value (r1) of sector parts of the center patch increases, the resonant frequency moves toward the high frequency band. This is because an

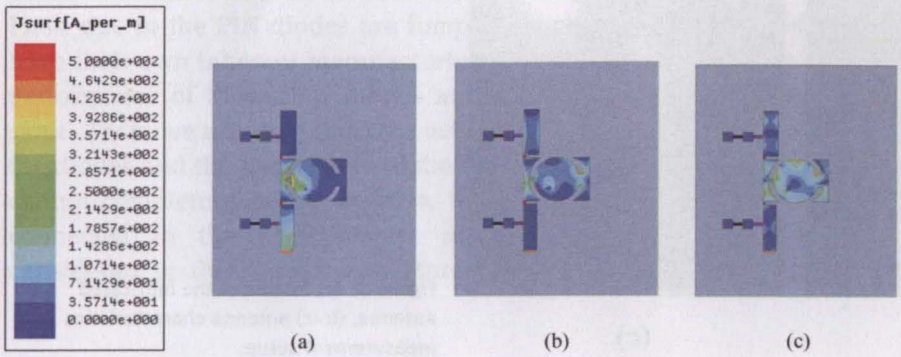

Figure 3: Current distribution of the proposed FRA working at (a) 11.3 GHz, (b) 16 GHz, and (c) 34 GHz.

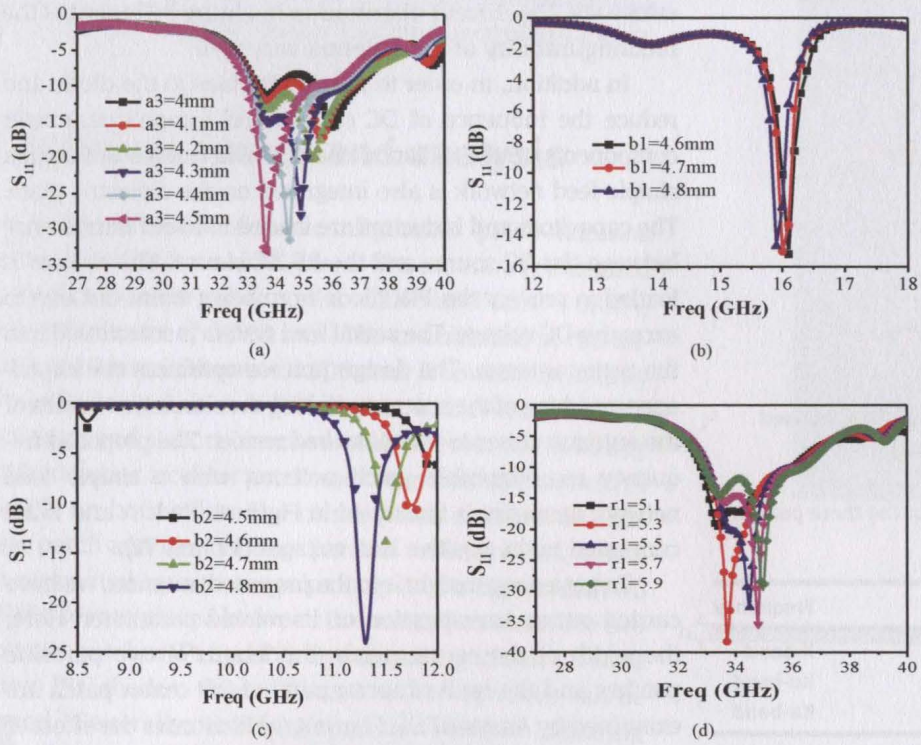

Figure 4: Simulated reflection coefficients (S_{11}) of the antenna for different (a) widths of the center patch *a3*, (b) lengths of the parasitic patch P1 (*b1*), (c) lengths of the parasitic patch P2 (*b2*), and (d) radii of sector parts of the center patch *r1*.

increase in the value of the radii (r1) can cause the overall size of the center patch to decrease.

3 Simulation and experimental results

The antenna is printed on a substrate with thickness of 0.508 mm and relative permittivity of 3.66. The antenna is simulated using full-wave solver Ansoft HFSS 15.0 and the fabricated antenna characteristics are measured using an Agilent N5244A vector network analyzer. A picture of the fabricated frequency reconfigurable patch antenna is shown in Figure 5. To accurately obtain the performance of the proposed reconfigurable antenna, the actual parameters of PIN diode are also included and considered in the simulation. PIN diodes are approximated as 5.2Ω resistors in the ON state and 0.015 pF capacitors in parallel with 10$k\Omega$ resistors in the OFF state.

Figure 6 (a)–(c) show the simulated and measured reflection coefficients (S11) versus frequency for states 1, 2, and 3, respectively. It can be seen that the operating

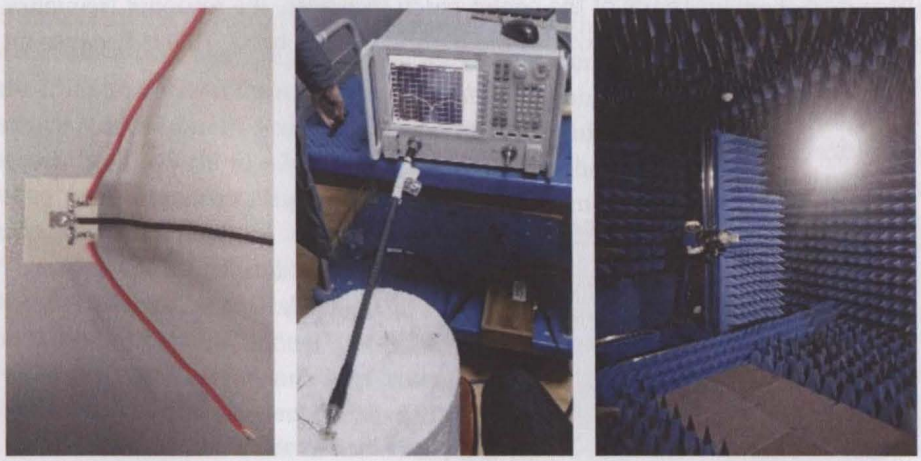

Figure 5: (a) Picture of the fabricated antenna, (b–c) antenna characteristics measurement setup.

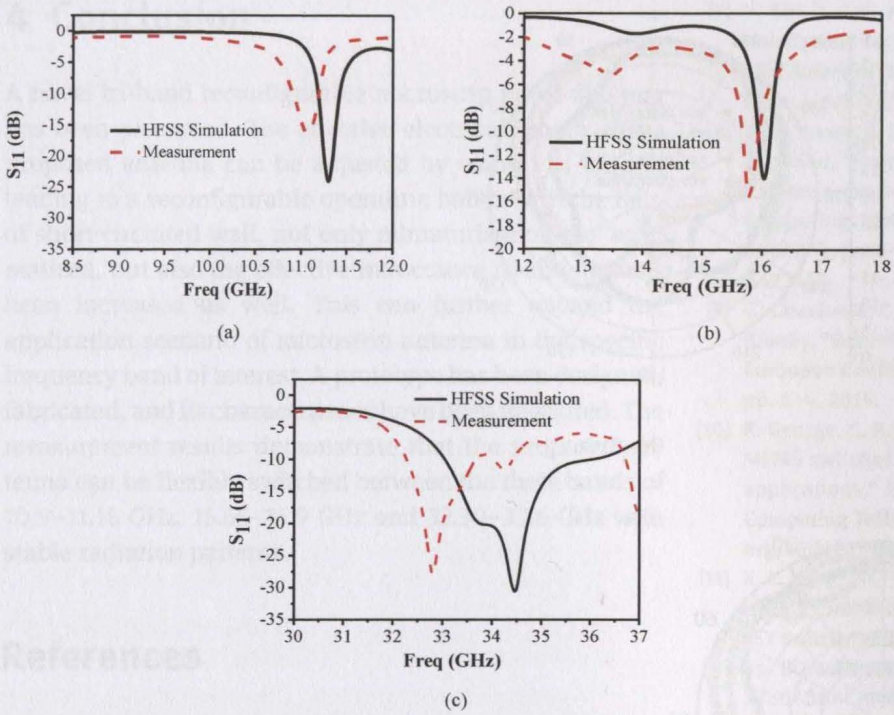

Figure 6: Simulated and measured reflection coefficients (S_{11}) of the prototype. (a) State 1, (b) State 2, and (c) State 3.

frequency bands of the antennas simulated in states 1–3 are 11.2–11.4 GHz, 15.9–16.2 GHz and 33–36 GHz, respectively. The measured working frequency bands are 10.9–11.18 GHz, 15.65–15.9 GHz, and 32.30–33.6 GHz, respectively. The measurement results and the simulation results are in good agreement.

To examine the proposed reconfigurable patch antenna, a microwave anechoic chamber is used to evaluate the normalized radiation patterns. The measured and simulated normalized radiation patterns in yoz-plane (E-plane) and xoz-plane (H-plane) are provided in Figure 7. Directional radiation patterns are observed at three different states. For convenience, the measurement and simulation reflection coefficients (S11) and peak realized gains of the proposed antenna at these three different states are summarized in Table 3. From Figure 6 and Table 3, it is seen that the measurement results slightly deviate from the simulation results. These differences can be attributed to several factors. First, due to the PIN diodes are lumped elements and have their own inherent manufacturing tolerances, the performance of those four diodes are not exactly the same. Then, we also find that, the actual parameters of the diodes and the parameters of the equivalent circuit cannot completely match. Besides, the long DC wires connected in the measurement process were not considered in the simulations. Moreover, due to the unavoidable tiny errors during the fabrication and assembly stages, together with the imperfections of the components (RF choke inductors and DC blocking capacitor) and the instability of dielectric constant of Rogers RO4350 substrate, the difference between the measured and simulated values is resulted. As shown in Figure 6 (c), we find that the difference between measured and simulated results for resonance frequency in Ka-band is a little high. In addition to the above reasons, it is known that in the Ka-band of millimeter wave band, the loss of dielectric substrate and conductor could also increase. Besides, we have also found that it is relatively sensitive to change the size in Ka-band, since small dimensional changes caused by machining and welding processes may result in significant impact on the working frequency points. Nevertheless, the measured and simulated results are reasonably consistent on the whole.

To further illustrate the superior performance of the designed antenna, a comparison between the proposed antenna and the design in previous works [13–16] is summarized in Table 4, in which λ_L is the free-space wavelength of the lowest operating frequency. It shows that the proposed antenna can achieve frequency reconfiguration in X-band, Ku-band, and Ka-band by controlling two PIN diodes, and realize directional radiation in these three frequency bands.

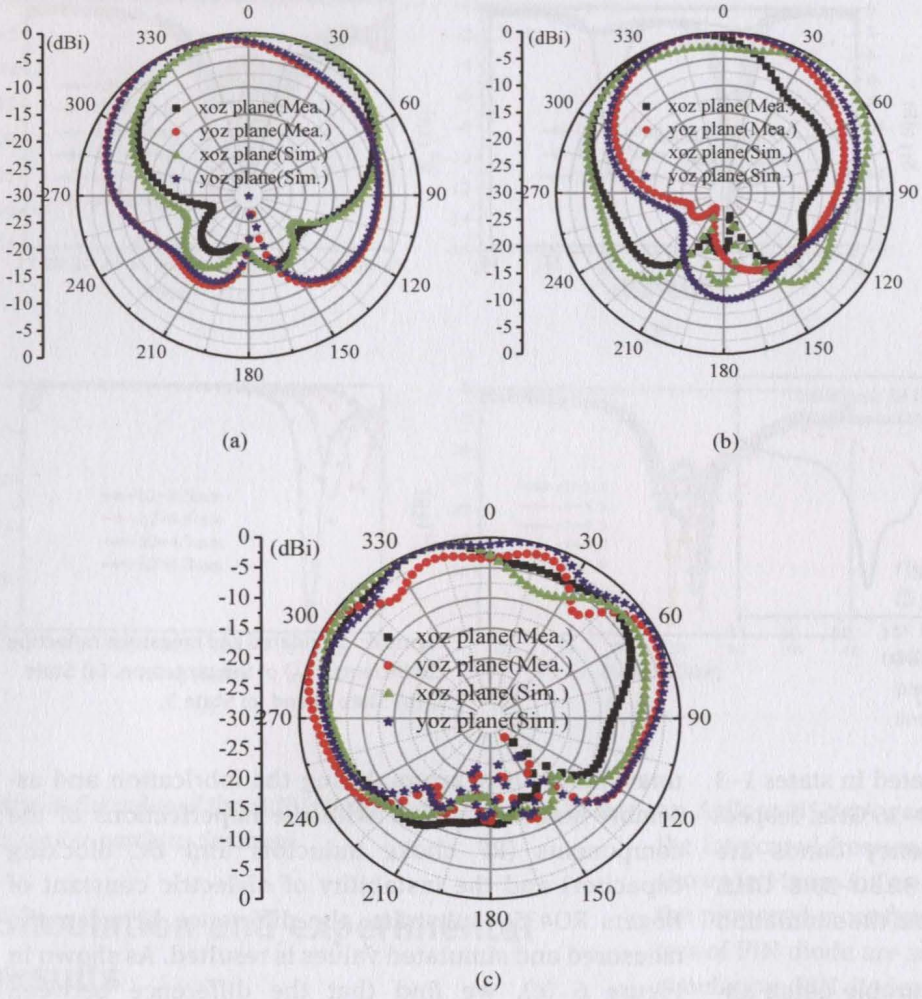

Figure 7: Measured and simulated normalized radiation patterns of the prototype. (a) State 1, (b) State 2, and (c) State 3.

Table 3: Measured and simulated performance characteristics of the proposed antenna.

State		1	2	3
Impedance range (GHz)	*Sim.*	11.2–11.4	15.9–16.2	33–36
	Mea.	10.9–11.18	15.65–15.9	32.3–33.6
Peak realized gain (dBi)	*Sim.*	0.9	6.9	8.12
	Mea.	0.2	5.3	7.65

Table 4: Performance comparison.

	Overall size (λ_L)	Number of PIN	Number of states	Central frequency of each state (GHz)	Radiation pattern
[13]	$0.28\lambda_L \times 0.28\lambda_L \times 0.01\lambda_L$	2	3	1.9/2.1/2.3	Omni-directional
[14]	$0.37\lambda_L \times 0.33\lambda_L \times 0.007\lambda_L$	6	3	2.36/3.34/5.3	Omni-directional
[15]	$0.24\lambda_L \times 0.26\lambda_L \times 0.015\lambda_L$	4	8	2.76/3.22/3.25/3.68/4.5/5.14 /6.36/7.68	Omni-directional
[16]	$1.22\lambda_L \times 0.87\lambda_L \times 0.11\lambda_L$	4	3	9.2/14.8/29.3	Directional
Pro.	$0.24\lambda_L \times 0.5\lambda_L \times 0.019\lambda_L$	2	3	11/15.8/33	Directional

4 Conclusion

A novel tri-band reconfigurable microstrip patch antenna has been presented. The effective electrical length of the proposed antenna can be adjusted by using PIN diodes, leading to a reconfigurable operating band. With the help of short-circuited wall, not only miniaturization has been realized, but also the effective inductance of antenna has been increased as well. This can further expand the application scenario of microstrip antenna in the specific frequency band of interest. A prototype has been designed, fabricated, and its characteristics have been measured. The measurement results demonstrate that the proposed antenna can be flexibly switched between the three bands of 10.9–11.18 GHz, 15.65–15.9 GHz and 32.30–33.6 GHz with stable radiation patterns.

References

[1] Y. Cai, Y. J. Guo, and T. S. Bird, "A frequency reconfigurable printed Yagi-Uda dipole antenna for cognitive radio applications," *IEEE Trans. Antennas Propag.*, vol. 60, no. 6, pp. 2905–2912, 2012. https://doi.org/10.1109/TAP.2012.2194654.

[2] S. Raman, P. Mohanan, N. Timmons, and J. Morrison, "Microstrip-fed pattern- and polarization-reconfigurable compact truncated monopole antenna," *IEEE Antennas Wireless Propag. Lett.*, vol. 12, pp. 710–713, 2013. https://doi.org/10.1109/LAWP.2013.2263983.

[3] H. Gu, J. P. Wang, and L. Ge, "Circularly polarized patch antenna with frequency reconfiguration," *IEEE Antennas Wireless Propag. Lett.*, vol. 14, pp. 1770–1773, 2015. https://doi.org/10.1109/LAWP.2015.2423321.

[4] M. C. Tang, Z. T. Wu, T. Shi, and R. W. Ziolkowski, "Electrically small, low-profile, planar, huygens dipole antenna with quad-polarization diversity," *IEEE Trans. Antennas Propag.*, vol. 66, pp. 6772–6780, 2018. https://doi.org/10.1109/TAP.2018.2869645.

[5] S. Ghosh and S. Lim, "A multifunctional reconfigurable frequency-selective surface using liquid-metal alloy," *IEEE Trans. Antennas Propag.*, vol. 66, pp. 4953–4957, 2018. https://doi.org/10.1109/TAP.2018.2851455.

[6] I. T. McMichael, "A mechanically reconfigurable patch antenna with polarization diversity," *IEEE Antennas Wireless Propag. Lett.*, vol. 17, pp. 1186–1189, 2018. https://doi.org/10.1109/LAWP.2018.2837902.

[7] Y. Shi, Y. Cai, X. F. Zhang, and K. Kang, "A simple tri-polarization reconfigurable magneto-electric dipole antenna," *IEEE Antennas Wireless Propag. Lett.*, vol. 17, pp. 291–294, 2018. https://doi.org/10.1109/LAWP.2017.2786945.

[8] W. A. Awan, A. Zaidi, N. Hussain, S. Khalid, Halima, and A. Baghdad, "Frequency reconfigurable patch antenna for millimeter wave applications," International Conference on Computing, Mathematics and Engineering Technologies (iCoMET), pp. 1–5, 2019. https://doi.org/10.1109/ICOMET.2019.8673417.

[9] G. Chaabane, C. Guines, M. Chatras, V. Madrangeas, and P. Blondy, "Reconfigurable PIFA antenna using RF MEMS switches," European Conference on Antennas and Propagation (EuCAP), pp. 1–4, 2015.

[10] R. George, C. R. S. Kumar, and S. A. Gangal, "Design of series RF MEMS switches suitable for reconfigurable antenna applications," International Conference on Circuit, Power and Computing Technologies (ICCPCT), pp. 1–5, 2017. https://doi.org/10.1109/TAP.2018.2851455.

[11] X. L. Yang, J. C. Lin, G. Chen, and F. L. Kong, "Frequency reconfigurable antenna for wireless communications using GaAs FET switch," *IEEE Antennas Wireless Propag. Lett.*, vol. 14, pp. 807–810, 2015. https://doi.org/10.1109/LAWP.2014.2380436.

[12] Z. J. Chen, I. Shoaib, Y. Yao, J. S. Yu, X.D.Chen, and C.G.Parini, "Pattern-reconfigurable dual-polarized dielectric resonator antenna," *IEEE Antennas Wireless Propag. Lett.*, vol. 15, pp. 1273–1276, 2016. https://doi.org/10.1109/LAWP.2015.2504585.

[13] H. A. Majid, M. K. A. Rahim, R. Dewan, and M. F. Ismail, "Frequency reconfigurable square ring slot antenna," 2015 IEEE International RF and Microwave Conference (RFM), pp. 147–150, 2015. https://doi.org/10.1109/RFM.2015.7587732.

[14] T. Li, H. Q. Zhai, X. Wang, L. Li, and C. H. Liang, "Frequency-reconfigurable bow-tie antenna for Bluetooth, WiMAX, and WLAN applications," *IEEE Antennas Wireless Propag. Lett.*, vol. 14, pp. 171–174, 2015. https://doi.org/10.1109/LAWP.2014.2359199.

[15] N. T. Selvi, R. Pandeeswari, P. T. Selvan, and A. Ranjan, "A selective frequency reconfigurable microstrip patch antenna using PIN diodes for cognitive radio applications," International Conference on Inventive Computing and Informatics (ICICI), pp. 980–984, 2017. https://doi.org/10.1109/ICICI.2017.8365284.

[16] L. Li, Z. Wu, K. Li, S. X. Yu, X. Wang, T. Li, et al., "Frequency-reconfigurable quasi-sierpinski antenna integrating with dual-band high-impedance surface," *IEEE Trans. Antennas Propag.*, vol. 62, pp. 4459–4467, 2014. https://doi.org/10.1109/TAP.2014.2331992.